Korean J. Chem. Eng., 38(8), 1727-1732 (2021)
DOI: 10.1007/s11814-021-0815-3

pISSN: 0256-1115
eISSN: 1975-7220

Esterification of free fatty acids in a rotor-stator spinning disc reactor

Yubin Wang*, Xiaoqiu Tao, Jun Li*,†, Siqi Zhang*, Yang Jin*, and Ming Chen***

*School of Chemical Engineering, Sichuan University, Chengdu, Sichuan 610065, P. R. China
**Sichuan Tobacco Quality Supervision and Testing Station, Chengdu, Sichuan 610041, P. R. China
(*Received 15 October 2020 • Revised 19 April 2021 • Accepted 23 April 2021*)

Abstract−Fatty acid methyl esters (FAMEs) were produced by the esterification of free fatty acids (FFA) with methanol, and sulfuric acid as the catalyst in a rotor-stator spinning disc reactor (RSSDR). The RSSDR, which shows excellent mixing efficiency and fast phase separation, was used as a novel continuous-flow esterification reactor. The influence of the variables (e.g., rotational speed, volume flow rate, rotor-stator distance, methanol-FFA molar ratio, catalyst dosage, and temperature) on esterification conversion (η) and productivity of FAMEs (P_{FAME}) were investigated. It was found that the experimental parameters have a great impact on the η and P_{FAME} in the RSSDR system, due to the effect of micromixing intensity and residence time distribution. Furthermore, to compare with other traditional esterification reactors, the values of η, P_{FAME}, and P_{FAME} per unit reactor volume (P_{FAME}/V_R) in the RSSDR were also employed to assess the performance for the production of FAMEs. It shows that the maximum values of P_{FAME}, and P_{FAME}/V_R attained were 0.14 mol/min and 3.06×10^{-2} mol/(mL min), respectively. Therefore, the RSSDR is proven to be an effective esterification reactor with high esterification conversion in comparison to conventional esterification reactors.

Keywords: Esterification, Rotor-stator Spinning Disc Reactor, Free Fatty Acid, Fatty Acid Methyl Esters

INTRODUCTION

The global energy crisis and climate change have recently become more and more severe because of CO_2 emissions and the increased demand for energy [1,2]. In recent years, biodiesel has become the focus of investigation due to its renewability and low CO_2 emission [3,4]. In addition, biodiesel is a non-toxic fuel. Because there is no sulfur and only about 11% oxygen by weight in biodiesel, resulting in a remarkable reduction of harmful emissions in comparison to petroleum fuel, especially of sulfur dioxide, particulate matter, unburned hydrocarbons and carbon monoxide [5]. Hence, biodiesel plays a key role in future energy production based on the above mentioned advantages.

Animal fats, vegetable oils, and microbial oils, which can be converted to fatty acid alkyl esters via an esterification reaction with alcohol and catalyst, are the raw materials of biodiesel [6]. As the concentration of free fatty acids (FFAs) in the oils has a significant influence on the production of biodiesel [7]. Most biodiesel is produced from edible oils with low FFA concentration, like palm oil, soybean oil, and rapeseed oil, which require fertilizer, are relatively high-cost, and even pose a serious threat to food crops for land [8-10]. Thus, to achieve the aim of economical and environment-friendly production of biodiesel, low-cost triacylglycerol feedstocks (e.g., waste frying oils and nonedible oils) are used as raw materials [11,12]. However, there are excessive amounts of FFAs contained in low-cost feedstocks, which would be saponified by the alkali catalysts employed in the process of transesterification, leading to difficulties in separation between the esters and glycerin, and also decreasing the yield of fatty acid methyl esters (FAMEs) [13,14]. As for the alkaline transesterification reactions, no more than 1 wt% FFAs should be contained in the feedstocks [15]. Thus, feedstocks with significant amount of FFAs should be pretreated to convert FFAs into biodiesel through the esterification process using an acid catalyst [16]. H_2SO_4 is regarded as one of the most common acid catalysts employed for the esterification reaction [13]. The transesterification reaction scheme is shown in Fig. 1.

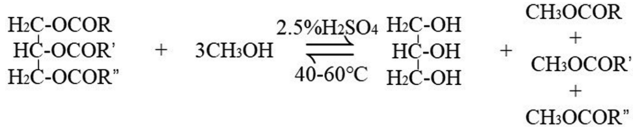

Fig. 1. The reaction scheme.

Traditional esterification reactors used for esterification process are commonly stirred tank reactors [17,18]. However, these reactors have some disadvantages, such as a long time ranging from one hour to several hours needed in the esterification process, high operating cost, and difficulty in process control [19]. To improve biodiesel conversion, decrease the reaction time and the process cost, several novel reactors have been proposed, including ultrasound reactor [20], microwave reactor [21], bubble column [22], and rotational packed bed [13]. Although these reactors are a significant improvement on biodiesel conversion and reaction time, there are various disadvantages presented in some of these reactors, such as low productivity, scale-up limitation, and high cost [21]. Therefore, the in-depth development of reactors with high productivity and biodiesel conversion is needed.

The rotor-stator spinning disc reactor has attracted a great deal of attention with its excellent mixing efficiency and mass transfer performance in recent years [23-26]. The RSSDRs are extensively

†To whom correspondence should be addressed.
E-mail: lijunlab@163.com

used in liquid-liquid systems [27,28], solid-liquid systems [29], and gas-liquid systems [30]. During the process of biodiesel production, the significant micromixing effect and the removal of reaction by-product water are the key to accelerate the esterification reaction and promise a high biodiesel conversion [31]. In the RSSDR, there is a rotor disc which can be operated to adjust the rotational speed, and a stator disc which is only a millimeters narrow gap from the rotor disc [32]. Due to the influence of shear force and centrifugal force in the narrow gap, where the reactants are contacted, the turbulence intensity, velocity gradient, and large specific surface area are generated to provide the excellent micromixing effect for the RSSDR. Note that the micromixing time in the RSSDR is evaluated to range from 10^{-5} to 10^{-3} s [33]. Furthermore, as a continuous-flow reactor, the residence time distribution of reactants in RSSDR is a few seconds [33], because the reactants are thrown outward to the housing cavity by the centrifugal force. And the reaction by-product water can be separated from the FAMEs by the high centrifugal force in the RSSDR [34]. Due to the advantages of structural characteristic and low cost, the RSSDR has been expected as a promising reactor to improve the esterification reaction conversion, and enhance biodiesel conversion performance, leading to achieving the goal of economic and industrialization of the biodiesel production.

Therefore, the objective of this work was to develop a novel technique for biodiesel production using the RSSDR as an esterification reactor, which also shows a new application of RSSDR in the area of biodiesel production. In this work, the esterification of the FFAs with methanol using sulfuric acid (H_2SO_4) as the catalyst in RSSDR was carried out. Methanol was chosen as the alcohol used in this work because it is the cheapest alcohol [13]. To evaluate the performance of the esterification reaction process, the influence of the variables such as rotational speed (N), volume flow rate of Oleic acid (Q_{FFA}), rotor-stator distance (H), methanol-FFA molar ratio (n_M/n_{FFA}), catalyst dosage based on the weight of oil (W_{cat}), and temperature (T) on the esterification conversion (η) and productivity of FAMEs (P_{FAME}) was investigated. Furthermore, to compare with other conventional esterification reactors, the values of η, P_{FAME}, and P_{FAME} per unit reactor volume (P_{FAME}/V_R) in the RSSDR were also employed to evaluate the performance of FAMEs.

EXPERIMENTAL

1. Material

High FFAs oleic acid was purchased from Kelong Chemical Co., Ltd. (Chengdu, China) with an acid of 146 mg NaOH/100 g, a density (ρ_{FFA}) of 0.896 g/mL and the average molecular weight of 282.5 g/mol. The methanol was bought from Changliao Chemical Co., Ltd. (Chengdu, China) with a density (ρ_{ML}) of 0.785 g/mL and the molecular weight of 32 g/mol and the boiling point of methanol is 64.9 °C. The H_2SO_4 (98.1% purity) used as the catalyst was also obtained from Changliao Chemical Co., Ltd. (Chengdu, China). The sodium hydroxide, Isopropyl alcohol, and absolute ether employed for analysis of the concentration of FFAs were produced by Kelong Chemical Co., Ltd. (Chengdu, China).

2. Setup and Procedure

The experimental setup employed for esterification of FFAs is displayed in Fig. 2. As shown there, it is obvious that RSSDR is a continuous-flow esterification reactor, leading to the time saving and production efficiency improvement compared to the stirred batch reactor. The experimental system mainly includes the RSSDR, storage tanks, constant flow pumps, motors, heaters, and stirrers. The specifications of the RSSDR are presented in Table 1.

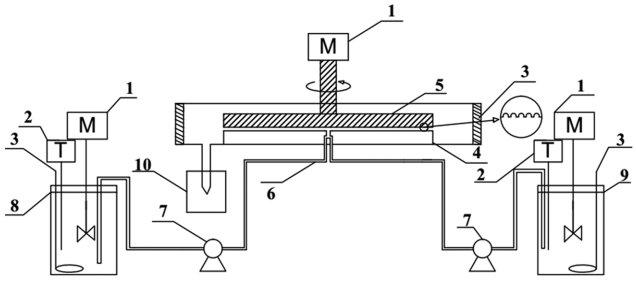

Fig. 2. Schematic drawing of the RSSDR set-up (1) motor, (2) thermocouple, (3) heater, (4) stator disc, (5) rotor disc, (6) pipe, (7) constant flow pump, (8) methanol-H_2SO_4 storage tank, (9) FFAs storage tank, and (10) collection bottle.

Table 1. Specification of the RSSDR and operating parameters used in this work

Items	Range of values
Geometrical parameters of RSSDR	
Radius of rotor disc (cm)	7.5
Radius of stator disc (cm)	7.5
Radial of kerve (cm)	19
Volume of the RSSDR (mL)	4.42-44.18
Operating parameters	
Rotational speed (rpm)	300-2,400
Volume flow rate of FFAs (mL/min)	5-50
Rotor-stator distance (mm)	0.25-2.50
n_M/n_{FFA}	2.97-23.77
W_{cat} (%)	0-20
T (°C)	20-60

The methanol and FFAs were stored in tanks. Based on a specific value of the catalyst dosage (W_{cat}, % w/w), a calculated amount of H_2SO_4 was added to the methanol before the experiments. During all of the experiments, the heat of methanol and FFAs was provided by the heaters. The temperature of the heaters was controlled by the PID controllers at preset values within ±1 °C. The RSSDR was wrapped in glass fiber heating tape (Guorui Thermal Control Electric Co., Ltd.) to control the temperature of the reactants throughout the system. The methanol and FFAs at the preset volume flow rates, which were controlled by the constant flow pump (CP1020, Sanwei Scientific Instrument Co., Ltd.), were simultaneously mixed prior to entering the rotor-stator cavity via the T-junction inlet in the center of the bottom stator disc. The liquids run from the center of the rotor-stator cavity to the periphery of the rotor-stator cavity due to the centrifugal force, and then the reaction products were collected by the collection bottle. All of the experimental parameters in this work are presented in Table 1. Every experiment was operated at atmospheric pressure, and every data was repeated three

times under steady state.

3. Analysis of Samples

To ensure complete phase separation, the reaction products were settled for 20 minutes at room temperature after they had been collected. To stop reaction occurring outside the reactor, the collect tube was pre-filled with iced deionized water. The sample was quenched in the collect tube by placing the tube into iced water [35]. Subsequently, the ester phase was washed three times with distilled water (water/ester phase volume ratio of 1) to remove residue such H_2SO_4, methanol [36,37]. After that, the ester phase was purified using the centrifuge (TG16-WS, Hunan Xiangyi Scientific Instrument Co., Ltd.) to remove the water. The concentration of FFA was calculated from the reduction of the acid value, which was determined by the titration of the samples according to the standard method GB/T 5530-2005 published by China National Standardization Management Committee.

4. Measurement of Biodiesel Production Performance

The reduction of acid value can be chosen to represent the esterification conversion by the following equation [38,39]:

$$\eta = \frac{FFA_i - FFA_e}{FFA_i} \times 100\% \quad (1)$$

where FFA_e represents the FFAs content at the end of the reaction. FFA_i is the initial FFA content.

The productivity of FAMEs (P_{FAME}) is defined as the following [13]:

$$P_{FAME} = Q_{FFA}\rho_{FFA}\eta/M_{FFA} \quad (2)$$

RESULTS AND DISCUSSION

1. Effects of Various Parameters on Biodiesel Production Performance

1-1. Effect of Rotational Speed

Fig. 3 illustrates η and P_{FAME} values as functions of N from 300 to 2,400 rpm at a fixed Q_{FFAs} of 20 mL/min, H of 0.25 mm, n_M/n_{FFA} of 11.89, W_{cat} of 10%, and T of 60 °C. It is clear that the values of η and P_{FAME} increase with the increase of N from 300 to 900 rpm. Whereas the values of η and P_{FAME} display an inverse trend with increasing N from 900 to 2,400 rpm. The similar trend where η and P_{FAME} vary with the N in RSSDR was also observed in the rotating packed bed, as reported by Chen et al. [13]. The explanation for this phenomenon may be depicted as follows. Due to the increase of the relative velocity between the discs and liquids, and the enhancement of turbulence at the liquids contact interface, the micromixing performance can be significantly intensified with increasing N from 300 to 900 rpm, resulting in the improvement of esterification conversion ability [33]. Nevertheless, the liquid velocity can be added with the increase of N, leading to the decrease of residence time of reactants in the rotor-stator cavity. The chance for the reactants to react decreases due to the reducing residence time, which plays a negative role in esterification conversion performance [40]. The decrease of residence time of the reactants becomes the primary factor with increasing N from 900 to 2,400 rpm, leading to the reducing of esterification conversion.

1-2. Effect of Volume Flow Rate

Fig. 4 displays the influence of Q_{FFA} from 5 to 50 mL/min on η and P_{FAME} at a fixed N of 900 rpm, H of 0.25 mm, n_M/n_{FFA} of 11.89, W_{cat} of 10%, and T of 60 °C. It is obvious that Q_{FFA} has a remarkable effect on η and P_{FAME}. An outstanding increase in η can be observed at Q_{FFA} from 5 to 20 mL/min and then a slight decrease in η is obtained when Q_{FFA} is higher than 20 mL/min. This is because the impinging velocity between the reactants can be increased with increasing Q_{FFA}, which has a positive effect on the renewal of the reactant contact interface and micromixing efficiency [40]. Mass transfer limitations play a negative role in the rate of reaction conversion. The way to eliminate the mass transfer limitation is to ensure that the micromixing rate is less than the kinetic reaction rate of the esterification of free fatty acids (about 10^{-3} s) [41]. In our previous work, we found that the micromixing time of RSSDR can be up to 10^{-5} s, which is less than the kinetic reaction rate of esterification of free fatty acids [33]. Therefore, RSSDR can minimize the mass transfer limitation on the esterification of free fatty acids reaction, leading to the significant im-

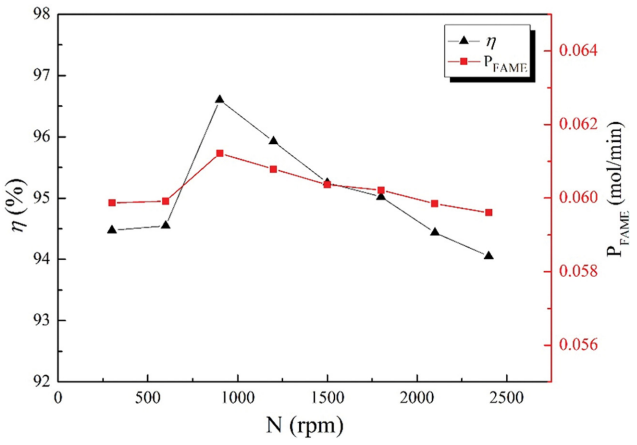

Fig. 3. Effect of rotational speed N on esterification conversion η and productivity of FAMEs P_{FAME}. Conditions: W_{cat}=10%, Q_{FFA}=20 mL/min, T=60 °C, n_M/n_{FFA}=11.89, and H=0.25 mm.

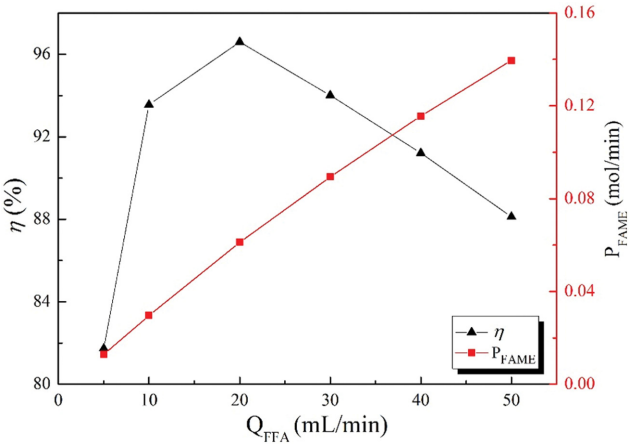

Fig. 4. Effect of volume flow rate of oleic acid Q_{FFA} on esterification conversion η and productivity of FAMEs P_{FAME}. Conditions: W_{cat}=10%, N=900 rpm, T=60 °C, n_M/n_{FFA}=11.89, and H=0.25 mm.

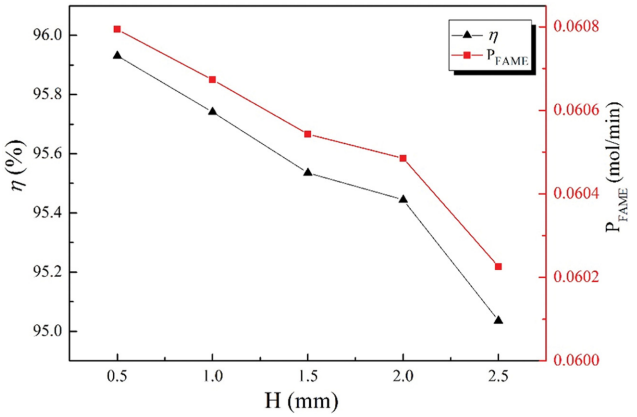

Fig. 5. Effect of rotor-stator distance H on esterification conversion η and productivity of FAMEs P_{FAME}. Conditions: W_{cat}=10%, N=900 rpm, T=60 °C, n_M/n_{FFA}=11.89, and Q_{FFA}=20 mL/min.

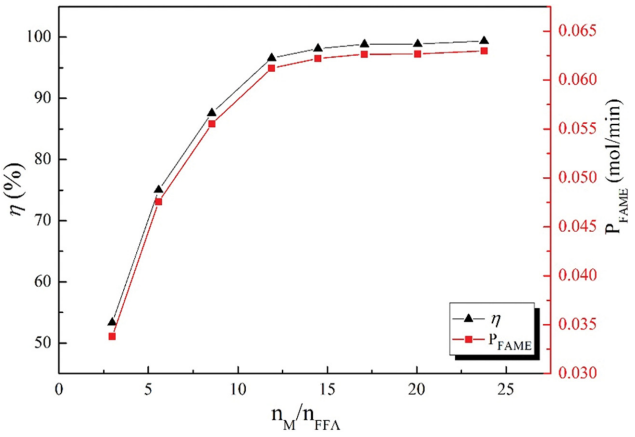

Fig. 6. Effect of n_M/n_{FFA} ratio on esterification conversion η and productivity of FAMEs P_{FAME}. Conditions: W_{cat}=10%, N=900 rpm, T=60 °C, H=0.25 mm, and Q_{FFA}=20 mL/min.

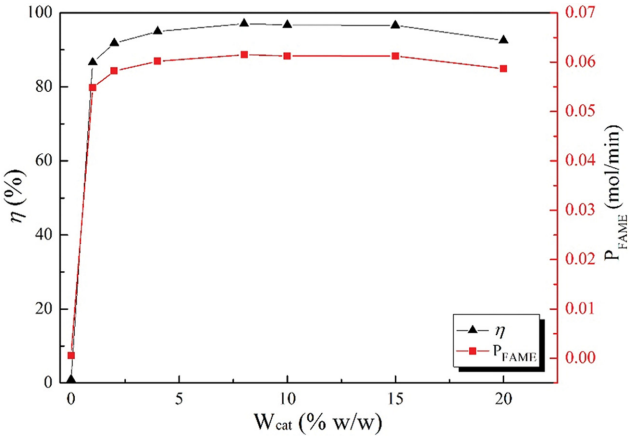

Fig. 7. Effect of catalyst dosage W_{cat} on esterification conversion η and productivity of FAMEs P_{FAME}. Conditions: n_M/n_{FFA}=11.89, N=900 rpm, T=60 °C, H=0.25 mm, and Q_{FFA}=20 mL/min.

provement of the esterification conversion performance. Meanwhile, the residence time of the reactants decreases with the increase of Q_{FFA}, which plays a negative role in the esterification conversion performance. The residence time of the reactants is a more principal factor than the renewal rate of interface in the esterification conversion performance with the Q_{FFA} over 20 mL/min [42].

It also can be seen that P_{FAME} increases as the increase of Q_{FFA} and the maximum value of P_{FAME} is up to 0.14 mol/min under the optimum experimental conditions. Based on Eq. (2), the P_{FAME} significant increases with larger Q_{FFAs} values due to the larger handling capacity of the Q_{FFA}.

1-3. Effect of Rotor-stator Distance

Fig. 5 shows the influence of varying H from 0.25 to 2.5 mm on η and P_{FAME} at a fixed N of 900 rpm, Q_{FFAs} of 20 mL/min, n_M/n_{FFA} of 11.89, W_{cat} of 10%, and T of 60 °C. It is clear that H has an important impact on the value of η and P_{FAME}. As H increases, both the value of η and P_{FAME} decrease. This may be caused by the reason that both the stator disc and rotor disc occur a boundary layer formed due to the increase of H, respectively [43]. Meanwhile, the two boundary layers are separated by a region which rotates with a constant tangential velocity. Therefore, due to the increase of H, the shear force in the rotor-stator cavity becomes weaker and weaker, resulting in a weaker turbulence and lower esterification conversion.

1-4. Effect of n_M/n_{FFA} Ratio

Fig. 6 depicts the variation of η and P_{FAME} with n_M/n_{FFA} from 2.97 to 23.77 at a fixed N of 900 rpm, Q_{FFAs} of 20 mL/min, H of 0.25 mm, W_{cat} of 10%, and T of 60 °C. A significant increase in η and P_{FAME} can be obtained with the increase of n_M/n_{FFA} from 2.97 to 11.89. And then a slight increase in η and P_{FAME} is obtained when the n_M/n_{FFA} is over 11.89. And the maximum value of η can be up to 99.37% under the optimum experimental conditions. The explanations for this phenomenon may be that based on the theoretical stoichiometry of the n_M/n_{FFA} ratio, the chemical equilibrium is driven toward the production of the esterification reaction with the increase of n_M/n_{FFA} ratio from 2.97 to 11.89, leading to an outstanding increase of the esterification conversion [44]. At the same time, the increase of n_M/n_{FFA} ratio means that the methanol increases too. Because methanol has an affinity with the hydrophilic stainless-steel rotor disc, the excess methanol may change the flow pattern of the liquids, resulting in the decrease of oleic acid in the rotor-stator cavity [45]. Thus, both the residence time of the oleic acid and micromixing efficiency would decline, which will slow the increase rate of the esterification conversion.

1-5. Effect of Catalyst Dosage

Fig. 7 shows η and P_{FAME} values as functions of W_{cat} between 0 and 20% at a fixed Q_{FFAs} of 20 mL/min, H of 0.25 mm, n_M/n_{FFA} of 11.89, N of 900 rpm, and T of 60 °C. It can be seen that η and P_{FAME} show an outstanding increase as W_{cat} increases from 0 to 1% and then has a moderate increase with the increase of W_{cat} between 1 to 8%. A slight decrease is obtained with W_{cat} over 8%. The correlation between η and W_{cat} in this work is a resemblance to that in another type of rotating reactor, as reported by Chen et al. [43]. This may be caused by the reasons that the active sites can be obtained to promote the reaction between methanol and oleic acid due to the addition of H_2SO_4 catalyst, leading to a significant increase in the esterification conversion. However, when the W_{cat} increases from 1 to 8%, the restriction of mass transfer within the

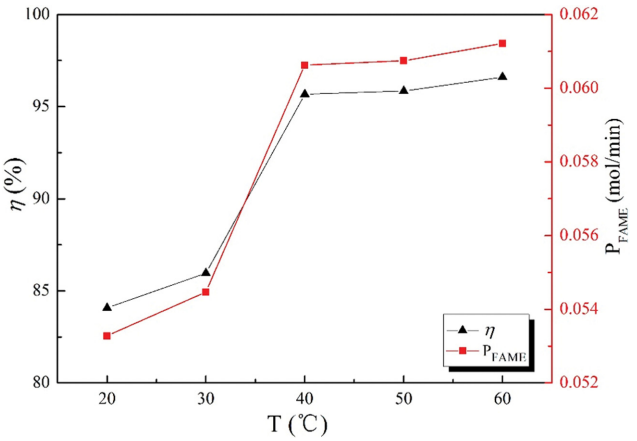

Fig. 8. Effect of temperature T on esterification conversion η and productivity of FAMEs P_{FAME}. Conditions: n_M/n_{FFA}=11.89, N=900 rpm, W_{cat}=10%, H=0.25 mm, and Q_{FFA}=20 mL/min.

reaction may play a negative role in the rate of reactants diffusion into H_2SO_4 active sites, resulting in a slight improvement in the esterification conversion. As H_2SO_4 over 8%, both the saturation and dilution effect of the catalyst may possibly occur. Thus, the esterification conversion shows a decline trend [13,46].

1-6. Effect of Temperature

Fig. 8 displays the variation of η and P_{FAME} with from 20 to 60 °C at a fixed N of 900 rpm, Q_{FFAs} of 20 mL/min, H of 0.25 mm, W_{cat} of 10%, and n_M/n_{FFA} of 11.89. It is clear that η and P_{FAME} have a remarkable improvement with the increase of temperature from 20 to 40 °C. It is because a higher esterification reaction rate can be obtained due to the increase of temperature. There is a slight increase in temperature, which increases from 40 to 60 °C. It may be that the vaporization of methanol has a negative effect on the esterification conversion due to the increase of temperature [45]. In addition, the solubility of reaction by-product water in the oleic acid may increase at the high temperature, which has an adverse effect on the improvement of the esterification conversion [13].

2. Comparison with other Esterification Reactors

The comparison of η, P_{FAME}, and P_{FAME}/V_R obtained in RSSDR with that of other esterification reactors is presented in Table 2. Note that the P_{FAME} value of the stirred batch reactor is calculated as $V_{FFA}\rho_{FFA}\eta/(M_{FFA}t_L)$, where V_{FFA} represents the volume of the FFA in this reactor [13]. It is obvious that the RSSDR has the highest P_{FAME}/V_R value among the esterification reactors. And the value of P_{FAME} is much higher than that of stirred batch reactor and adsorption column. It means that the RSSDR has super productivity and esterification conversion ability than the other esterification reactors. Furthermore, the RSSDR also shows advantages such as simple operation and low cost. Consequently, the RSSDR turns out to be a promising process intensification equipment for biodiesel production.

CONCLUSION

The process of esterification of FFA in a continuous-flow esterification reactor named RSSDR was investigated, with the methanol-oleic acid reaction as working system. Preliminary research was carried out on the influence of various parameters, such as rotational speed, volume flow rate, rotor-stator distance, methanol-FFA molar ratio, catalyst dosage, and temperature on esterification conversion and productivity of FAMEs. It was found that these parameters have a significant impact on the esterification conversion and the maximum value of P_{FAME}, and P_{FAME}/V_R can up to 0.14 mol/min and 3.06×10^{-2} mol/(mL min), respectively. In addition, based on the value of esterification conversion, productivity of FAMEs and its per unit reactor volume, the esterification conversion performance of RSSDR was compared with that of other esterification reactors. It has been proved that the RSSDR shows higher esterification performance than the other conventional esterification reactors, which means that the RSSDR has a broad application prospect in biodiesel production.

ACKNOWLEDGEMENT

This work was supported by the National Natural Science Foundation of China (No. 21776180).

NOMENCLATURE

H : rotor-stator distance [mm]

Table 2. Comparison of esterification conversion ability with other reactors

Ref.	Reactor	Chemical system	Catalyst	n_M/n_{FFA}	W_{cat} (% w/w)	T (°C)	η (%)	P_{FAME} (mol/min)	$P_{FAME}/V_R\times10^3$ (mol/(mL min))
13	Rotational packed reactor	Oleic acid-ethanol	H_2SO_4	2.5-33.7	0-29.1	21-60	10.0-96.6	0.042-1.20	0.171-4.88
14	Fixed-bed reactor packed	Oleic acid-methanol	H_2SO_4	18.5	2-10	60	69.9-97.5	0.0003-0.00046	0.0075-0.0114
16	Adsorption column	Oleic acid-methanol	H_2SO_4	3-9	0.5-10	90-110	61.2-99.7	0.006-0.009	0.058-0.087
17	Stirred batch reactor	Oleic acid-methanol	H_2SO_4	4.2-10.1	1.0-5.1	35-55	84.4-96.9	0.0008-0.00095	0.0016-0.0019
18	Stirred batch reactor	Palm fatty acids-methanol	H_2SO_4	3	0-0.1	130	20.4-93.8	0.004-0.07	0.001-0.003
20	Ultrasonic reactor	Oleic acid-methanol	H_2SO_4	5-9	1.0-5.0	90-110	62.2-95.4	0.020-0.149	0.002-0.015
Present study	RSSDR	Oleic acid-methanol	H_2SO_4	2.97-23.77	0-20	20-60	0.95-99.4	0.0006-0.14	0.14-31.60

M_{FFA} : average molecular weight of FFA [g/mol]
N : rotational speed [rpm]
n_{FFA} : FFA molar mass [mol]
n_M : methanol molar mass [mol]
P_{FAME} : productivity of FAMEs [mol/min]
Q_{FFA} : volume flow rate of Oleic acid [mL/min]
T : temperature [°C]
t_L : residence time in reactor [min]
V_R : volume of the reactor [mL]
W_{cat} : catalyst dosage based on the weight of oil [% w/w]

Greek Letters

ρ_{FFA} : density of FFA [g/mL]
ρ_M : density of methanol [g/mL]
η : esterification conversion [%]

REFERENCES

1. Z. H. Li, P. H. Lin, J. C. S. Wu, Y. T. Huang, K. S. Lin and K. C. W. Wu, *Chem. Eng. J.*, **234**, 9 (2013).
2. F. Moazeni, Y. C. Chen and G. S. Zhang, *J. Clean. Prod.*, **216**, 117 (2019).
3. M. Sanchez-Cantu, L. M. Perez-Diaz, M. Morales-Tellez, I. Martinez-Santamaria, J. C. Hilario-Martinez and J. Sandoval-Ramirez, *Fuel*, **189**, 436 (2017).
4. Z. E. Tang, S. Lim, Y. L. Pang, H. C. Ong and K. T. Lee, *Renew. Sust. Energ. Rev.*, **92**, 235 (2018).
5. E. Sendzikiene, V. Makareviciene and P. Janulis, *Renew. Energ.*, **31**, 2505 (2006).
6. L. Zhang, M. Xian, Y. C. He, L. Z. Li, J. M. Yang, S. T. Yu and X. Xu, *Bioresour. Technol.*, **100**, 4368 (2009).
7. T. M. Mata, F. Pinto, N. Caetano and A. A. Martins, *J. Clean. Prod.*, **184**, 481 (2018).
8. L. K. dos Santos, R. R. Hatanaka, J. E. de Oliveira and D. L. Flumignan, *Renew. Energ.*, **130**, 633 (2019).
9. E. D. C. Cavalcanti, E. C. G. Aguieiras, P. R. da Silva, J. G. Duarte, E. P. Cipolatti, R. Fernandez-Lafuente, J. A. C. da Silva and D. M. G. Freire, *Fuel*, **215**, 705 (2018).
10. D. C. Boffito, C. Pirola, F. Galli, A. Di Michele and C. L. Bianchi, *Fuel*, **108**, 612 (2013).
11. A. Talebian-Kiakalaieh, N. A. S. Amin and H. Mazaheri, *Appl. Energ.*, **104**, 683 (2013).
12. R. D. Souza, T. Vats, A. Chattree and P. F. Siril, *Catal. Lett.*, **148**, 2848 (2018).
13. Y. H. Chen, L. C. Wang, C. H. Tsai and N. C. Shang, *Ind. Eng. Chem. Res.*, **49**, 4117 (2010).
14. J. Ni and F. C. Meunier, *Appl. Catal. a-Gen.*, **333**, 122 (2007).
15. M. Canakci and J. Van Gerpen, *T. Asae*, **44**, 1429 (2001).
16. I. L. Lucena, G. F. Silva and F. A. N. Fernandes, *Ind. Eng. Chem. Res.*, **47**, 6885 (2008).
17. J. M. Marchetti and A. F. Errazu, *Biomass. Bioenerg.*, **32**, 892 (2008).
18. D. A. G. Aranda, R. T. P. Santos, N. C. O. Tapanes, A. L. D. Ramos and O. A. C. Antunes, *Catal. Lett.*, **122**, 20 (2008).
19. Z. Z. Wen, X. H. Yu, S. T. Tu, J. Y. Yan and E. Dahlquist, *Bioresour. Technol.*, **100**, 3054 (2009).
20. V. G. Deshmane, P. R. Gogate and A. B. Pandit, *Ind. Eng. Chem. Res.*, **48**, 7923 (2009).
21. I. Choedkiatsakul, K. Ngaosuwan, S. Assabumrungrat, S. Tabasso and G. Cravotto, *Biomass. Bioenerg.*, **77**, 186 (2015).
22. C. J. Stacy, C. A. Melick and R. A. Caimcross, *Fuel. Process. Technol.*, **124**, 70 (2014).
23. M. Meeuwse, J. van der Schaaf, B. F. M. Kuster and J. C. Schouten, *Chem. Eng. Sci.*, **65**, 466 (2010).
24. Y. B. Wang, J. Li, Y. Jin, M. Chen and R. Ma, *Chem. Eng. Process.*, **149**, 107834 (2020).
25. E. R. van Kouwen, W. Winkenwerder, Z. Brentzel, B. Joyce, T. Pagano, S. Jovic, G. Bargeman and J. van der Schaaf, *Chem. Eng. Process.*, **160**, 108303 (2021).
26. K. Julia and O. Hinrichsen, *Chem. Eng. Process.*, **136**, 152 (2019).
27. F. Visscher, J. van der Schaaf, M. H. J. M. de Croon and J. C. Schouten, *Chem. Eng. J.*, **185**, 267 (2012).
28. Y. B. Wang, J. Li, Y. Jin, J. H. Luo, Y. Cao and M. Chen, *Sep. Purif. Technol.*, **207**, 158 (2018).
29. P. G. Mendoza, S. J. C. Weusten, M. T. de Groot, J. T. F. Keurentjes, J. C. Schouten and J. van der Schaaf, *Int. J. Heat. Mass. Tran.*, **104**, 650 (2017).
30. M. Meeuwse, E. Hamming, J. van der Schaaf and J. C. Schouten, *Chem. Eng. Process.*, **50** 1095 (2011).
31. I. L. Lucena, R. M. A. Saboya, J. F. G. Oliveira, M. L. Rodrigues, A. E. B. Torres, C. L. Cavalcante, E. J. S. Parente, G. F. Silva and F. A. N. Fernandes, *Fuel*, **90**, 902 (2011).
32. Y. B. Wang, J. Li, Y. Jin, M. Chen, Y. Cao and J. H. Luo, *Chinese J. Chem. Eng.*, **27**, 2643 (2019).
33. Y. B. Wang, J. Li, Y. Jin, J. H. Luo, M. Chen and C. Yan, *Chem. Eng. J.*, **362**, 357 (2019).
34. Y. B Wang, M. Chen, Y. Jin, Y. Ouguang and J. Li, *J. Taiwan Inst. Chem. Eng.*, **115**, 20 (2020).
35. Z. Qiu, J. Petera and L. R. Weatherley, *Chem. Eng. J.*, **210**, 597 (2012).
36. A. Chaudhuri, K. P. L. Kuijpers, R. B. J. Hendrix, P. Shivaprasd, J. A. Hacking, E. A. C. Emanuelsson, T. Noël and J. van der Schaaf, *Chem. Eng. J.*, **400**, 15 (2020).
37. M. Berrios and R. L. Skelton, *Chem. Eng. J.*, **144**, 459 (2008).
38. D. C. Boffito, F. Galli, C. Pirola, C. L. Bianchi and G. S. Patience, *Ultrason. Sonochem.*, **21**, 1969 (2014).
39. S. Photaworn, C. Tongurai and S. Kungsanunt, *Chem. Eng. Process.*, **118**, 1 (2017).
40. H. J. Yang, G. W. Chu, J. W. Zhang, Z. G. Shen and J. F. Chen, *Ind. Eng. Chem. Res.*, **44**, 7730 (2005).
41. J. P. Lopes, S. S. S. Cardoso and A. E. Rodrigues, *Chem. Eng. J.*, **176-177**, 3 (2011).
42. K. Yang, G. W. Chu, L. Shao, Y. Luo and J. F. Chen, *Chem. Eng. J.*, **153**, 222 (2009).
43. F. Haseidl, J. Pottbacker and O. Hinrichsen, *Chem. Eng. Process.*, **104**, 181 (2016).
44. Y. H. Chen, Y. H. Huang, R. H. Lin and N. C. Shang, *Bioresour. Technol.*, **101**, 668 (2010).
45. L. Boulange-Petermann, C. Gabet and B. Baroux, *Colloid Surface A.*, **272**, 56 (2006).
46. N. M. Yunus, S. Z. Abidin and C. S. Yee, *Energ. Source. Part A.*, **40**, 2518 (2018).